

Ungani Oil Field, Canning Basin – Evaluation of a Dolomite Reservoir

David Long*
Buru Energy
16 Ord Street, West Perth 6005
DavidLong@buruenergy.com

Amy Millar
Buru Energy
16 Ord Street, West Perth 6005
AmyMillar@buruenergy.com

Stuart Weston
Weston Petroleum Consulting
Address
stuart@westonpetroleumconsulting.com.au

Lionel Esteban
CSIRO-Energy
26 Dick Perry Av, Kensington 6152
Lionel.Esteban@csiro.au

Anne Forbes
Chemostrat
1131 Hay St, West Perth 6005
Anneforbes@chemostrat.com

Martin Kennedy
MSK Scientific Pty Ltd
85 Aristrade Avenue, Kallaroo 6025
mkennpet@aol.com

SUMMARY

Core supported study of the heterogeneous Ungani dolomite reservoir architecture is driving development drilling and upgrades to field resource estimates. Vuggy connected and macro non-connected pore space was directly measured over a 70m continuous core using 3D structural analysis of CT-scans. Plug density measurements indicate non-connected or sub-140 micron resolution contribution of around 1% to 2.5% (pu) for the tight matrix, but all remaining porosity potentially contributes to oil production. The high resolution core porosity data is vertically repositioned and upscaled to calibrate neutron-density and sonic petrophysically derived porosities which are inadequate to resolve productive zones using conventional reservoir cut-offs. Conditioned resistivity image data correlated exceptionally with directly measured connected porosities. Reservoir properties were extrapolated to all wells across the Ungani field giving field net/gross estimates of up to 63% and porosities over 30% pu in some vuggy and brecciated zones. The heterogeneity and prolific nature of the uppermost 17m of reservoir had not been previously recognised due to poor log data coverage and access at the casing points. Recent re-analysis of this section at Ungani-3 with Chemostrat ICP-OES-MS analysis of ditch cuttings was instrumental in proposing additional drilling to re-target this zone. Mineralogy analysis is used to calculate rock grain densities and help calibrate neutron-density derived porosity logs over the Ungani field. Up-scaled core porosity correlates well with density and sonic porosity logs. Resistivity logs adjusted for mineralogy can also be used to predict porosity and support the use of resistivity image logs to identify vuggy zones and estimate porosity at a higher resolution than conventional logging tools. A field static model was populated with three facies distributed over vertical zones according to the distribution encountered in the core porosity analysis and well logs, and iteratively matched to the dynamic pressure data and field production history which exhibits field scale multi-Darcy horizontal permeability and protection from vertical water cut. Further drilling and downhole artificial lift is planned to extend field production rates to 3000 bbls/day. Increased confidence in this regionally developed reservoir is supporting further exploration of undrilled prospects in this immature and under-explored trend

Key words: Ungani, Dolomite, Core, CT-scan, Connected Porosity

INTRODUCTION

The Ungani field was discovered in the Canning Basin in 2011, 100km east of Broome. 37°API oil was recovered from Tournasian aged (Lower Laurel) dolomite reservoirs (Edwards and Streitberg 2013) developed on the crest of a Devonian compressional anticline and located within an under-explored 200km wide play fairway on the southwest flank of the Fitzroy Trough (Figure 1). The Ungani structure comprises a number of fault blocks with oil recovered from each of the four existing wells, and further development wells due to be drilled in late 2017 (Figure 2). Despite inter-well interference demonstrating multi Darcy permeability and well initial rates over 1500bopd, petrophysical estimates of total porosity were only 6% to 9%, while limited core and rock data indicated a tight matrix with porosity of only 1% to 2%. The image log data indicate a heterogeneous pore system and the existence of vug and macro porosity zones. Resource estimates were compromised by a poor understanding of the static data, specifically where to apply petrophysical cut-offs and the relative contribution of connected versus low permeability or non-connected pore space. Dynamic modelling and production wells interference data were consistent with much larger recoverable volumes.

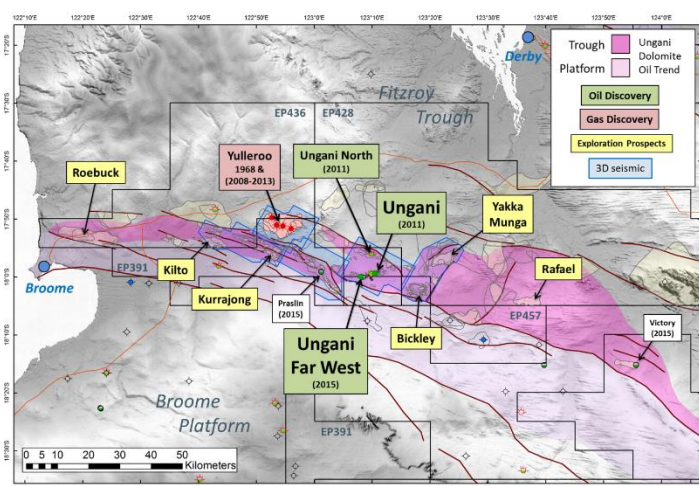


Figure 1: Early wells were shallow or were located on the Broome Platform and terraces. Discovery of oil in dolomites at Ungani 150km east of Broome in 2011 has opened a 200km long oil exploration fairway on the flanks of the Fitzroy Trough with only a handful of wells, all of which have recovered light oil.

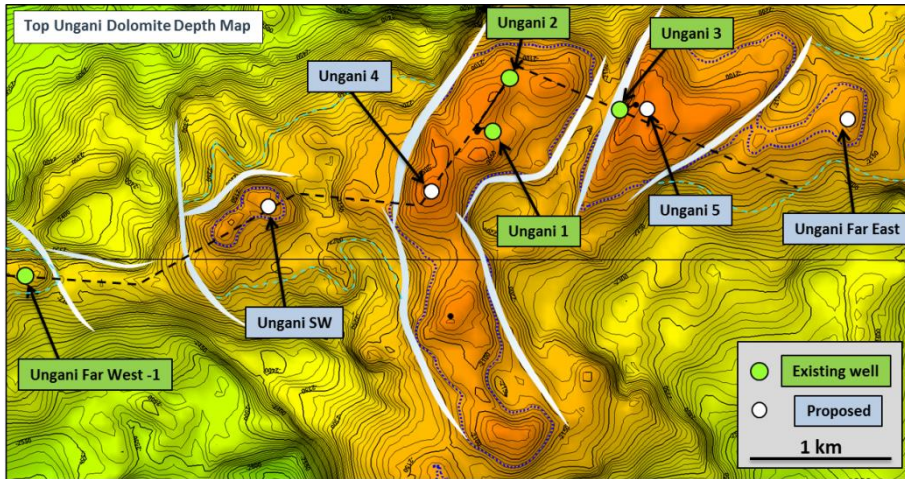
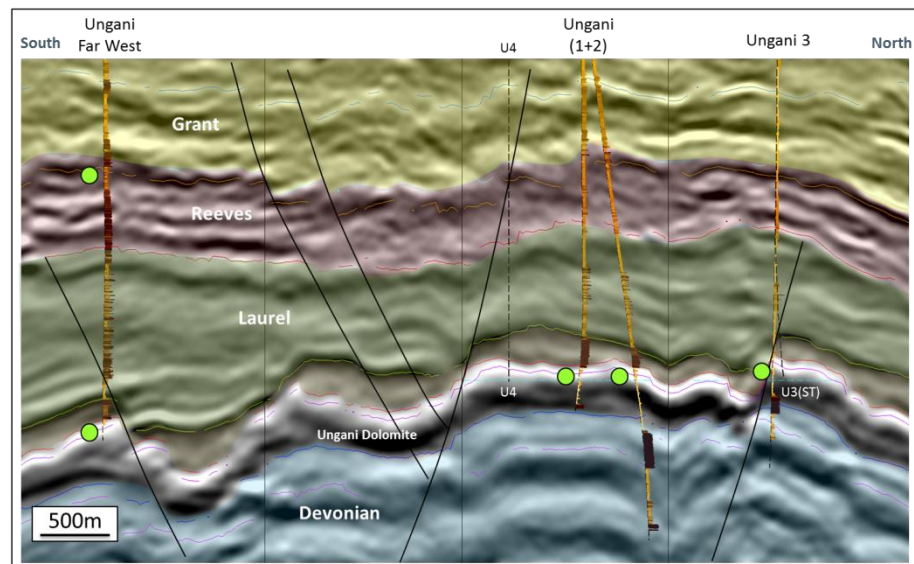


Figure 2: Ungani field depth map of the top of the Ungani Dolomite Reservoir mapped on 3D seismic.

The overlying Laurel sealing shale is reactive, the instability of which resulted in the need for a production side track of discovery well Ungani-1. The requirement to fully penetrate and isolate this formation in each well has resulted in typically up to 20m of the upper most part of the reservoir being set behind casing, where the evaluation is compromised by incomplete log coverage. The Ungani-3 appraisal well targeted a separate (eastern) fault block using

newly acquired 3D seismic. The well trajectory cuts the fault removing most of the overlying Laurel shale section. Recent correlation work suggests the uppermost section of reservoir was again isolated behind casing which took significant losses during cementing operations. Although field-wide aquifer pressure communication was established, the remaining exposed section of reservoir at Ungani-3 failed to produce at attractive rates.

Figure 3: Arbitrary 3D seismic line over the Ungani field wells Ungani-1(ST) and Ungani-3. The core porosity and reservoir evaluation supports the proposal to drill Ungani-4 and Ungani-5 development wells



The Praslin well, drilled on the Jurgurra Terrace in 2015, confirmed aerial extent of reservoir with a prolific vug porosity zone within the upper 20m of the reservoir. In late 2015 the Ungani Far West well targeted a separate oil bearing structure 4km west of the Ungani facility. A 70m wireline retrievable core from the Laurel shale and Ungani Dolomite reservoir (93% recovery) was acquired, revealing insights into the Ungani dolomite

reservoir porosity system, the contribution of connected and non-connected porosity to production contribution and field reserves; the short-comings of existing log resolution, and; a realisation of significant missed opportunities in the Ungani field itself.

UNGANI FAR WEST CORE ANALYSIS

HQ (2.5" diameter) core acquisition at Ungani Far West was achieved using the DDH1 rig#31 mineral coring rig over 26 runs each recovering intervals of typically 3 to 6 metres. 60 micron pixel photography and 3D spectral images were acquired at Corescan for mineralogy and to support oversized thin section and stable isotope petrographic studies. Core to logging depth alignment is achieved by correlating the top reservoir interface and geological features such as a conductive pyrite filled fracture. High porosity zones and core loss intervals can be immediately correlated with zones of respective low density and high neutron- density separation, slow sonic and lower resistivity, and appreciable drilling fluid losses despite being drilled with balanced mud weights (Figure 4).

In geo-materials studies CT scanning is applied to view full-diameter sample sections to determine orientation relative to bedding and the presence of discontinuities and specifically in this example, for pore quantification. A Medical X-ray CT scan of the complete core was conducted at CSIRO using a Siemens SOMATOM definition AS in order to measure the total and macro-connected porosity over the 6cm diameter core dimensions. An energy beam of 140kV/300mAs with a helical acquisition (0.35mm pitch) was applied to acquire the high resolution three-dimensional model by stacking contiguous cross-sectional two-dimensional images every 0.4mm (slice thickness) with a XCT voxel size resolution of 0.1mm (x and y axis). This generates a classical x-ray image in DICOM format reconstructed using an H50s algorithm from Siemens to restrict noise and beam hardening artefacts. Due to the vuggy and occasionally broken nature of the reservoir section and to retain original orientation and depth, scanning was conducted using the full core tray (i.e. 4 cores) without moving/disturbing the cores.

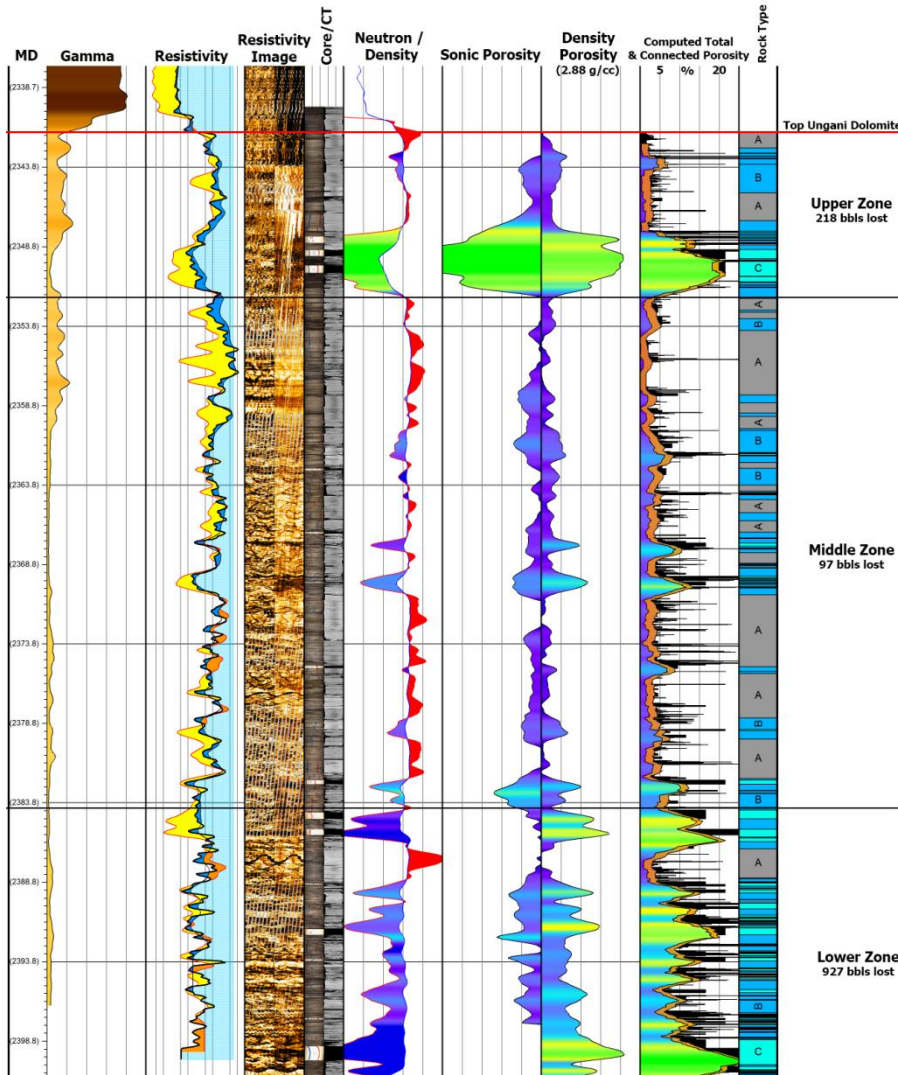


Figure 4: The Ungani Far West continuous core achieved with 93% recovery. Despite mud weights close to balance, over 1300 bbls mud filtrate were lost to the formation primarily over high porosity upper and lower zones. Measured core porosities are upscaled from 0.4mm to 72cm (green log) and the average amplitude scaled back to the neutron-density calculated porosity (coloured curve).

Interference between the cores caused variable attenuation and noise on the XCT images particularly in the XZ direction (Figure 5). Additional signal processing and filtering was successful at measuring the pore space but at a slightly reduced resolution of 140 μm (0.14mm) Since X-ray attenuation of the CT-scan pixel is a function of the density and atomic number of the material being analysed (Wellington and Vinegar 1987), it is possible to compute the bulk density profile along the core CT profile and directly convert to porosity with an appropriate calibration using solid reference minerals such as dolomite. The mean CT value was computed for each transverse image away from the edge of the sample in order to eliminate possible beam-hardening artefacts (10cm² green circled area). The mean CT value was computed for each transversal CT image and

calibrated with grain density values derived from independent core plug measurements for additional accuracy (rather than using pure dolomite crystal for calibration). The pore spaces greater than 140 μm were segmented to compute “total macro” porosity and directly assess the connectivity over the core dimensions.

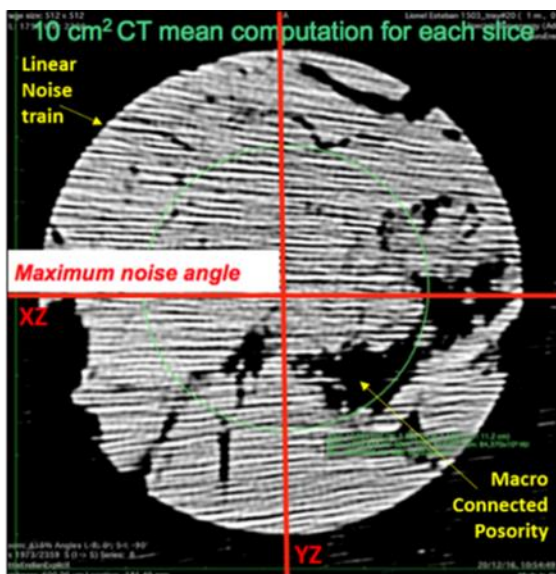


Figure 5: An unfiltered XCT transverse view of the core showing the noise train generated by signal interference between multiple cores.

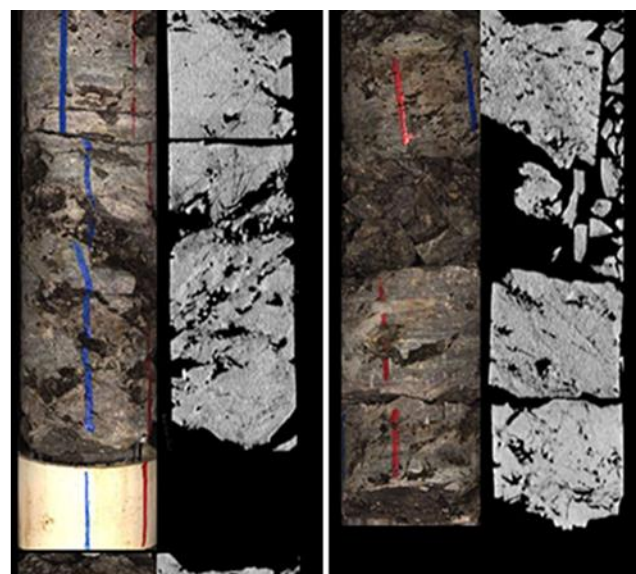


Figure 6: Ungani Far West core CT scan images recorded as slice number and assigned to wireline loggers depth by geological features to the core photography.

Noise filtered sub-volumes and computed 1D digital data of total and connected porosity for each respective slice were then exported for fully intact portions of the core - typically around 2300 individual XCT slices per 95cm core interval resulting in a total of more than 160,000 image slices over all of the core material. Significant manual interaction was required to accurately assign a depth to each slice by matching distinctive geological features (fractures, vugs, and pyritic veins and nodules) on the core scan images with the depth matched high resolution core photography while accounting for missing section and core movement in the trays (Figure 6).

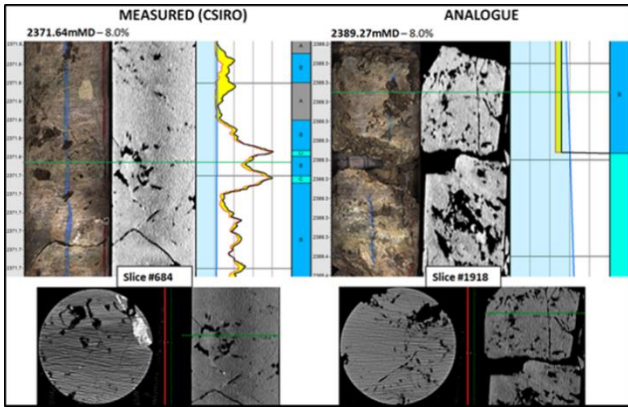


Figure 7 Porosities for sections of core which could not be directly calculated were manually derived through analogue.

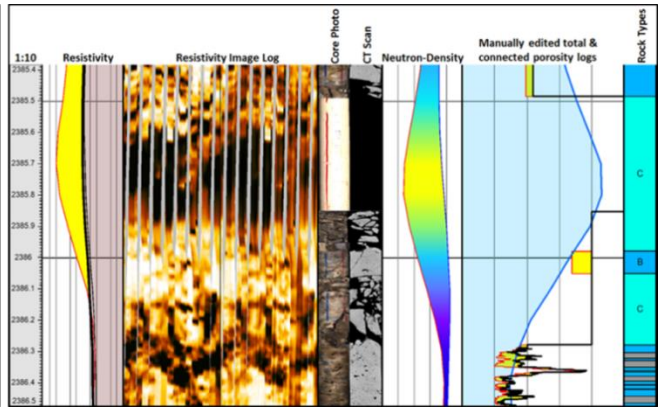
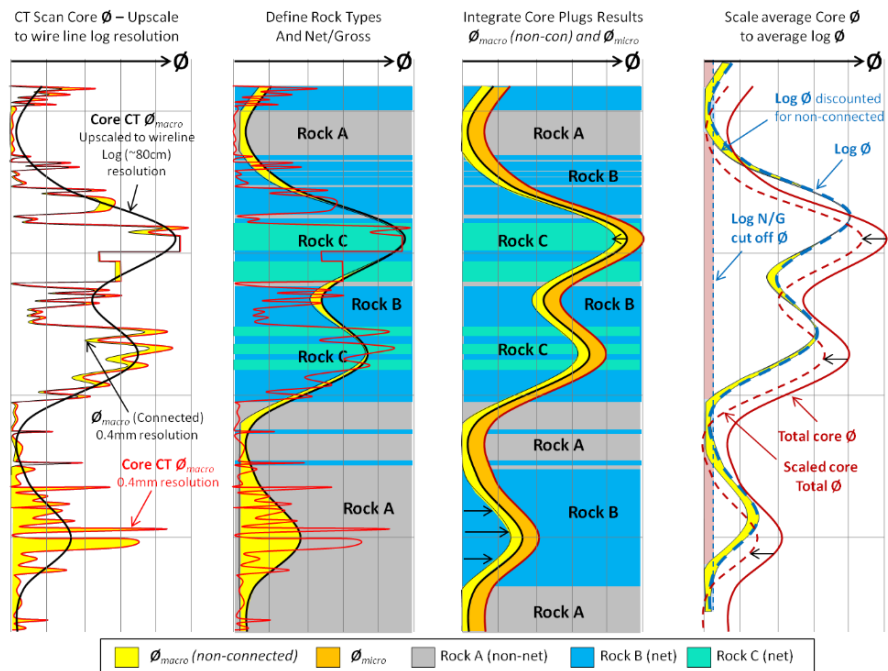


Figure 8: Lost core zones were estimated by comparison to image logs where typically significant conductive zones coincide with mud losses and poor core recovery.

Core to scan image matching were conducted over a 30cm window with each slice number attributed an equivalent logging depth. The effective stretch is less than 1%, leading to slice intervals typically between 0.396 and 0.404mm. The computed 1D total and connected porosity data was resampled to a 0.4mm sample interval and scaled to 72cm (non-weighted) by generating a running average over 1800 data-points so it could be directly compared with the conventional petrophysical porosity logs (Figure 7). Where the core was partly broken (such as rubble or highly fractured rock) and direct computation of porosity from XCT scans would not be reliable, a manual estimation of porosity was conducted by detailed study of the orthogonal and slice images using computed porosity examples as a direct analogue (Figure 8).

Short intervals of core loss could typically be correlated with high porosity / vug zones at the base of each core run where coring failed. Comparison of these directly measured core porosities and the borehole resistivity images confirmed the relationship between conductive zones and effective porosity over a half centimetre pad-tool resolution. Core loss zones generally coincide with zones of significant porosity - also characteristic of low densities, low resistivity, and often mud losses during coring operations where the magnitude was estimated by comparing and matching the non-weighted average total porosity to the conventional neutron-density derived log (Figure 9). Intervals with high conductivity and high densities correlating with minerals such as pyrite were excluded.

Figure 9 Calibrating log porosity ϕ_{macro} (connected) from core, up-scaled from a 0.4mm resolution. Three rock facies types are used to describe the porosity system. The total porosity is adjusted by the non-connected porosity contribution (in yellow) which also defines cut off for net/gross estimates. The non resolved porosity (less than 140 μ m) is shown in orange). Amplitude scaling can be applied to reduce the average core porosity to the equivalent log estimates.



For the purposes of this study, the large scale “vuggy” and connected (macro) porosity contributions were combined and defined as pore space that could be resolved by the scan images (>0.14mm). “Micro” porosity is defined as the non-resolvable contribution estimates which were backed out from routine core plug analysis (Figure 10). We can describe the total porosity as:

$$\phi (\text{Total}) = \phi_{macro} (\text{connected}) + \phi_{macro} (\text{non-connected}) + \phi_{micro}$$

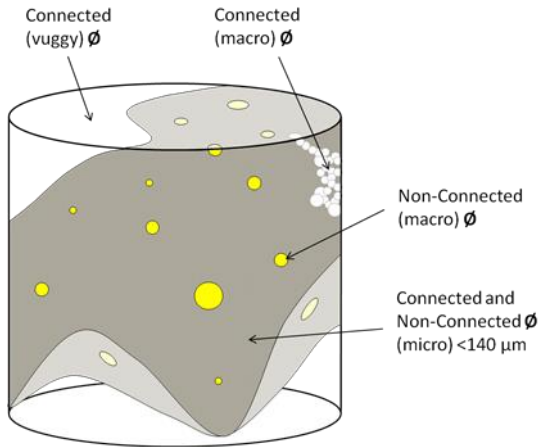


Figure 10: Scan porosity was attributed to non-connected (coloured yellow), were re-attributed as plug measurements measured over 10% connected porosity with 1D permeability

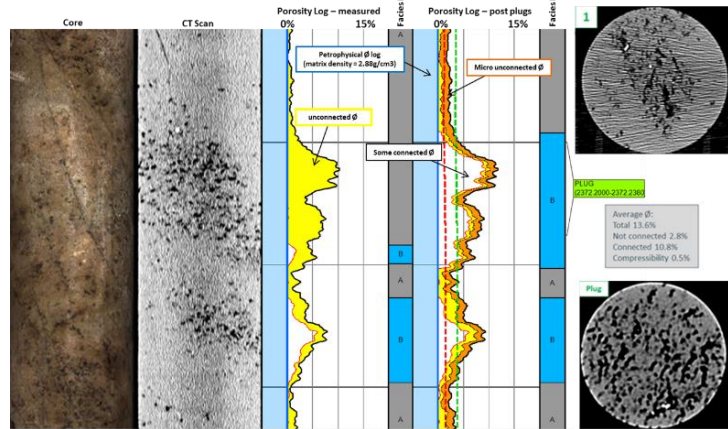
composition and rock diagenesis. Nitrogen gas bulk porosity-permeability measurements under confining pressures from 500 to 4000 psi were greater than suggested by both the CT scan and density log evaluation, and also highlighted sections where the core analysis had incorrectly defined porosity (with up to 10% p.u.) as non-connected (Figure 11).

Figure 11: Pore space distribution in the Ungani Dolomite has both vug, macro and sub-resolvable (micro) contributions. The section was redesignated as “C-type” rock and assigned a core average non-connected porosity contribution of 2.4% (coloured in orange). The core plug CT scan image is shown as a comparison to the core CT transverse slice.

The core plug total non-connected porosity from the difference in the plug grain and bulk densities is calculated to average 2.4% p.u. which compares with only 0.6% p.u. estimated from the CT scan. The remaining 1.8% p.u. can be attributed to the unresolved (non-connected) micro porosity (ϕ_{micro}) as shown in Table 1.

Table 1: Core derived rock type ratio, N/G of 61% and total porosity of 11.1% which is discounted 1.8% to give non-connected pore space.

Although it is quite possible that the micro porosity (ϕ_{micro}) may also be connected (as routine plug analysis suggest), this is difficult to quantify and is assumed to be zero. To best represent the heterogeneity, the reservoir is classified into three rock facies types: A) Poor, B) Moderate, and C) Excellent and for which net/gross, and an effective porosity and permeability distribution could be derived. Type A Rock is defined as having little or no connected porosity (0 to 1%), with any greater porosity calculated to be isolated. With plug measured permeability below 1mD, and with negligible shale content across the reservoir section, rock type A represents the non-net section. Type B rock has some connected macro porosity (3% to 10% p.u.) and permeability from 1-420mD, with no significant vugs. Rock C has significant connected porosity comprising a network of vugs or open fractures with estimated porosities locally in excess of 20% and permeability in the range 250-7000mD. This type dominates well flow rates. Regular core plug measurements of grain density enabled calibration of the XCT scan analysis and the wireline neutron-density log calculations of porosity. Background tight rock densities of 2.90 g/cc were observed due to the presence of dispersed heavy minerals but were as low as 2.80 g/cc in vuggy zones (type C rock) possibly influenced by the presence of oil or local changes in mineral



Rock Type	Total Average		Average Macro ϕ			Micro ϕ = 2.4% minus Macro ϕ (non connected)
	Net Rock	Total ϕ	Total	Connected	non-connected	
C	20%	21.2%	18.9%	10.0%	2.3%	21.2%
B	41%	6.0%	4.5%	3.6%	0.9%	1.5%
A	39%	2.5%	60.0%	10.0%	50.0%	1.9%
B+C	61%	11.1%	9.3%	8.7%	0.6%	1.8%
TOTAL	100%	7.7%	5.9%	5.3%	0.6%	1.8%

Well chemostratigraphy correlation (Ratcliffe et al 2010) was performed using ditch cuttings and core chips samples using high precision elemental data collected for 50 elements by Inductively Coupled Plasma – Optical Emission Spectroscopy – Mass Spectrometry (ICP-OES-MS, Jarvis and Jarvis 1992a & b). Elemental data was also used for a chemostratigraphic correlation giving information on bulk lithology and a fingerprint of clastic provenance (e.g. Ti/Nb) as well as changes in diagenesis (e.g. Ca/Sr and S) to distinguish between the Ungani dolomite reservoir and the overlying Upper Laurel carbonates (Figure 12). The reservoir is correlated from the Ungani Far West core to the Ungani-1 and Ungani-2 wells using a 3 layer reservoir model comprising a 17m thick upper zone of mostly vuggy excellent porosity, a 35m thick middle zone of generally poor or modest porosity, and a thick lower zone with modest to good porosities. The correlation to Ungani-3 had previously been uncertain due to the apparent absence of both the Laurel sealing shale and the upper vuggy zone. Evaluation of reprocessed Ungani 3D seismic suggests the Ungani-3 well trajectory crosses the footwall bounding fault in the Laurel (Figure 3). The lowermost 20m 12-1/4” hole section cemented behind the 9-5/8” casing (where 110bbls cement losses were reported) has a chemostratigraphic fingerprint of the Ungani Dolomite, and the interval just 5m shallower can be correlated to an equivalent interval 90m shallower in the Upper Laurel Carbonates at Ungani-2. A re-examination of the pulsed neutron through casing logs indicate we have found the missing vuggy reservoir section with estimates of over 10% porosity. Mineralogy analysis confirm average grain densities of 2.85g/cc in Ungani-1, 2 and 3 and 2.88g/cc in Ungani Far West and correlate with the MgO concentration which suggests dolomite vs siliciclastic mineralogy is a controlling factor. The ICP calculated densities are consistent with those measured on ditch cuttings in Ungani-2, and were used to recalibrate the Ungani wells neutron-density estimated porosities.

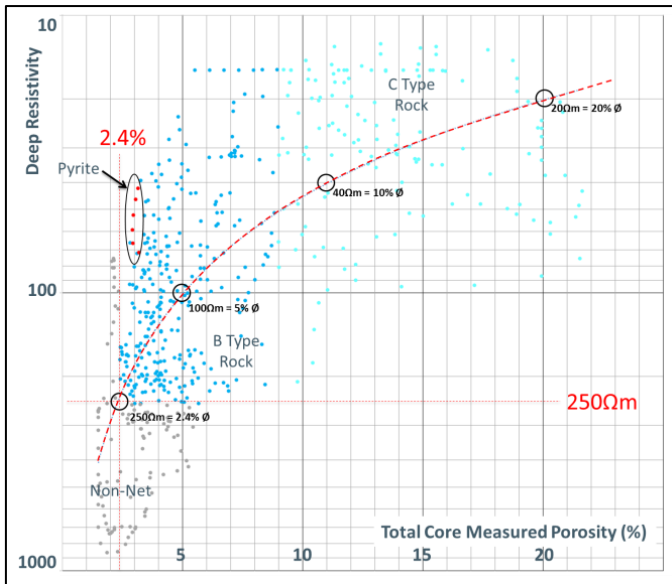


Figure 14: A good inverse correlation is observed between the deep resistivity log and measured core porosity

Up-scaled core measured porosity was cross plotted against log derived values based on density and sonic log estimates. Due to the heterogeneous nature of the reservoir, very tight matrix rock and large vugs with filtrate invasion and no mud cake, the resistivity log was also demonstrated to be a reliable porosity indicator once the occasional mineralogical anomalies had been removed (Figure 14). This strongly supports the approach that treats conductive zones on the resistivity logs as evidence of pore space, although quantitative methods are subject to a halo effect. Connected (net contributing) porosity can then be estimated by discounting the total log porosity by 1.8% p.u.

A 50x50x0.5m PETREL static model populated with the adjusted well reservoir parameters was used in an interactive dynamic modelling exercise to match the production history (pressures, fluid rates and water-cut) at Ungani (Figure 15). Minor vertical permeability (K_v) is required to

allow for modest vertical water migration. The model horizontal permeability (K_h) contains intervals reaching multi Darcy in the Upper reservoir zone. It is based on plug measurements and adjusted slightly to fit the production dynamic history match (Figure 16). Original formation test pressure data acquired below the Ungani oil contact at Ungani demonstrated a common, normally pressured water gradient across the Greater Ungani Area. Static gradient surveys from the UFW 1 Upper zone show minor pressure depletion immediately after the flow test, but subsequent recharge that is consistent with Ungani field wells. A shifted water gradient established at Ungani Far West (4 km to the west) and an oil column pressure at Ungani-3 both were consistent with the field pressure depletion, confirming the presence of a well-connected and permeable regional aquifer.

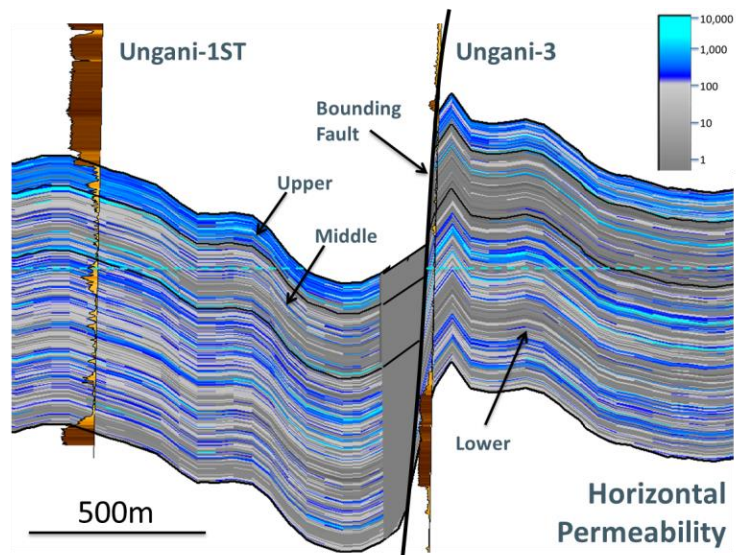


Figure 15: Static model cross section showing the rock facies types (left) and permeability (right) distributed over the 3 Reservoir layers

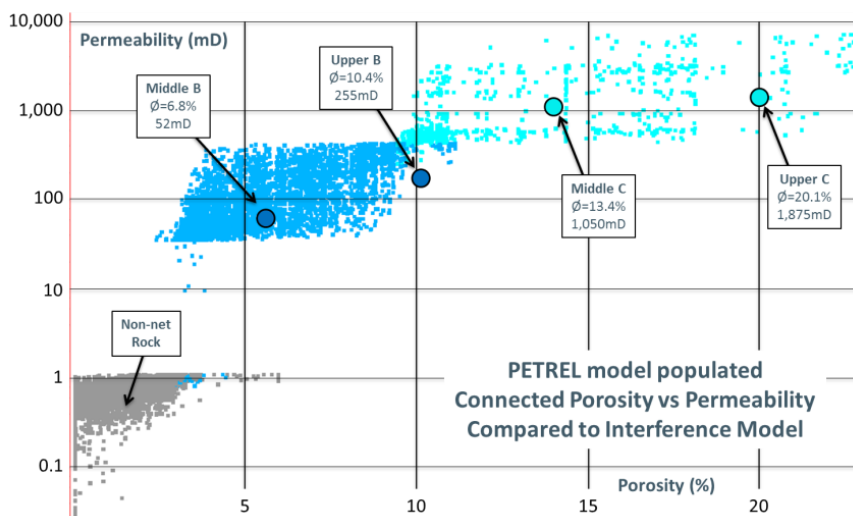


Figure 16: Porosity and Permeability relationship used in the reservoir modelling and respective values derived from the well interference tests in Ungani field.

Ungani 2 and Ungani 3 in April 2016 show some recharge of reservoir pressure post Jan 2016 shut in of field – but not to original reservoir pressure. Natural field pressure depletion after 600,000bbl of production, together with material balance calculations confirm the presence of an extensive but benign aquifer. The modest but slowly increasing water cut is likely sourced from expansion and a low energy flank water ingress. Down hole ESP pumps are being fitted to wells to provide artificial lift. As oil prices recovered, production in the field was restarted in 2017. As part of the start up procedure a pulsed interference test of 10 hour pulses followed by 14 hour shut ins was conducted over a 5 day period.

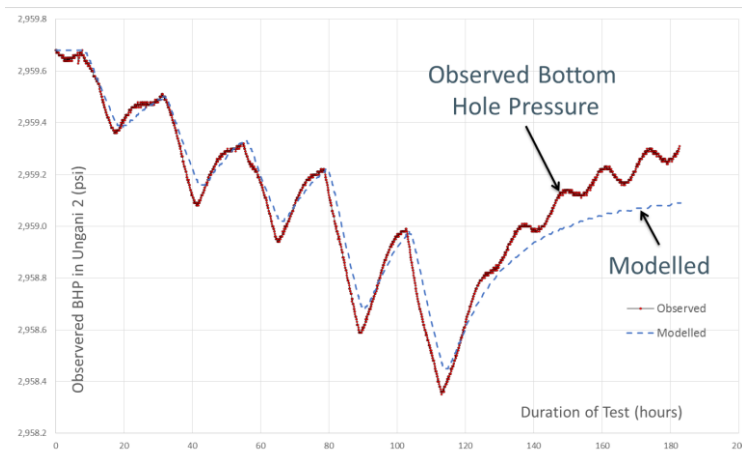


Figure 17: Well interference in the Ungani reservoir for build-ups tests in Ungani-1. The pressure wave is transmitted over 400m to downhole static gauges in Ungani-2. The rock facies reservoir model based on the core porosity analysis and used for production history matching was shows a near perfect match to the actual data.

Ungani IST1 was used as the producing well with Ungani 2 located 580m away observing the pressure response within minutes, indicative of a highly connected porosity system. A series of radial flow models have been created with the average properties from the core work being applied and data from the Upper and Middle reservoir zones. These matched the observed start up interference data with excellent results (Figures 16 and 17) demonstrating that the model are indeed representative of the bulk of the

porosity/permeability derived from this study when applied in the dynamic reservoir between the two wells.

CONCLUSIONS

Ungani Dolomite reservoir connected porosity, directly measured at a high resolution from CT-scanning and calibrated with plug measurements, demonstrate that the conventional logs under-estimate total porosities and do not resolve the reservoir heterogeneity. The non-contributing fraction of porosity is measured to be between 1% and 2.4% p.u. which is used to define petrophysical cut-off for non-net rock. Chemostratigraphic analyses were successful in correlating reservoir sections and identifying missed oil pay. Mineralogy analysis is used to calculate rock grain densities and help calibrate neutron-density derived porosity logs over the Ungani field. Up-scaled core porosity correlates well with density and sonic porosity logs. Resistivity logs adjusted for mineralogy can also be used to predict porosity and support the use of resistivity image logs to identify vuggy zones and estimate porosity at a higher resolution than conventional logging tools. Three rock facies types and three reservoir zones are used to describe the net/gross and populate a reservoir model with porosities and permeability that are confidently correlated to well interference data and match oil field production history. Hence direct core measurements have built confidence in dynamic pressure and interference data to accurately represent the macro scale reservoir better than the Ungani field wells log derived reservoir Net/Gross and porosities.

ACKNOWLEDGMENTS

The authors would like to thank Buru Energy for allowing publication of this study, Corescan, Chemostrat, and CSIRO and contributions from Buru geoscientists, past and present. We also acknowledge the Karajarri Yanj and Nyikina Mangala communities, traditional owners of the land where Ungani wells are drilled.

REFERENCES

- Edwards, P., and Streitberg, E., 2013, Have We Deciphered the Canning? Discovery of the Ungani Oil Field: West Australian Basins Symposium 2013.
- Jarvis, I. & Jarvis, K.E., 1992a. Inductively coupled plasma-atomic emission spectrometry in exploration geochemistry. In: Hall, G.E.M. (ed.), *Geoanalysis. Journal of Geochemical Exploration*, **44**, 139 - 200.
- Jarvis, I. & Jarvis, K.E., 1992b. Plasma spectrometry in earth sciences: techniques, applications and future trends. In: Jarvis, I. & Jarvis, K.E. (eds), *Plasma Spectrometry in Earth Sciences. Chemical Geology*, **95**, 1 - 33.
- Jones S.C., 1972, A rapid accurate unsteady-state Klinkenberg permeameter, *SPE* 3535: 383-397.
- Klinkenberg L.J., 1941, The permeability of porous media to liquid and gases. *API Drill. Prod. Pract.* **41**: 200–213.
- Pervukhina M., Gurevich B., Dewhurst D.N., and Siggins A.F., 2010, Experimental verification of the physical nature of velocity-stress relationship for isotropic porous rocks, *Geophysical Journal International*, **181**: 1473–1479.
- Ratcliffe, K.T., Wright, A.M., Montgomery, P., Palfrey, A., Vonk, A., Vermeulen, J. & Barrett, M., 2010. Application of chemostratigraphy to the Mungaroo Formation, the Gorgon Field, offshore Northwest Australia. *APPEA Journal 2010: 50th Anniversary Issue*, 371 - 385.
- Shapiro S.A., 2003, Elastic piezosensitivity of porous and fractured rocks, *Geophysics*, **68(2)**: 482-486.
- Wellington, S. and Vinegar, H., 1987, X-ray computerized tomography, *Journal of Petroleum Technology*, **39**: 885-898
- Wu Y-S, Pruess K., and Persoff P., 1998, Gas flow in porous media with Klinkenberg effects. *Transport in Porous Media* **32**: 117-137.